2-Oxazoline/benzoxazole-1,10-phenanthrolinylmetal (iron, cobalt or nickel) dichloride: Synthesis, characterization and their catalytic reactivity for the ethylene oligomerization

Min Zhang [a], Rong Gao [a], Xiang Hao [a], Wen-Hua Sun [a,b,*]

[a] Key Laboratory of Engineering Plastics and Beijing National Laboratory for Molecular Sciences, Institute of Chemistry, Chinese Academy of Sciences, Beijing 100190, China
[b] State Key Laboratory for Oxo Synthesis and Selective Oxidation, Lanzhou Institute of Chemical Physics, Chinese Academy of Sciences, Lanzhou 730000, China

ARTICLE INFO

ABSTRACT

Series of 2-benzoxazole-1,10-phenanthrolines (**L1**–**L4**) and 2-oxazoline-1,10-phenanthrolines (**L5**–**L8**) were synthesized and used as tridentate N^N^N ligands in coordinating with metal (nickel, cobalt or iron) chlorides. Their metal complexes, nickel(II) (**Ni1**–**Ni8**), cobalt(II) (**Co1**–**Co8**) and iron(II) (**Fe1**–**Fe8**), were characterized by elemental and IR spectroscopic analyses. The molecular structures of the ligand **L2** and the complexes **Ni3**, **Co1**, **Co3** and **Fe2** have been determined by the single-crystal crystallography. The nickel complex **Ni3** and iron complex **Fe2** display an octahedral geometry, whereas cobalt complex **Co1** is with a distorted bipyramidal geometry and **Co3** as square pyramidal geometry. At 10 atm ethylene, all the complexes showed good activities in ethylene dimerization upon activation with appropriate aluminum cocatalysts; the nickel complexes gave the activity up to 3.11×10^6 g mol^{-1}(Ni) h^{-1} upon activation with diethylaluminum chloride (Et$_2$AlCl), meanwhile the cobalt and iron complexes showed activities up to 1.51×10^6 g mol^{-1}(Co) h^{-1} and 1.89×10^6 g mol^{-1}(Fe) h^{-1}, individually, upon activation with modified methylaluminoxane (MMAO).

© 2008 Elsevier B.V. All rights reserved.

1. Introduction

The major chemical industry of about 6 million tons of α-olefins provides basic feedstocks for detergents, lubricant, plasticizers and also the comonomers in the copolymerization with ethylene for the linear low-density polyethylene (LLDPE) [1–3]. Late transition metal complexes have demonstrated the feature of importance in ethylene oligomerization with the practicing catalyst represented by the nickel complexes in the Shell higher olefin process (SHOP) [4–9]. In the past decade, late-transition metal complexes in olefin reactivity have been greatly attracted because of the initial works of cationic α-diimino nickel and palladium complexes by Brookhart group [10] and bis(imino)pyridinyl iron and cobalt complexes by Brookhart [11] and Gibson groups [12], individually. Inspired with SHOP process for ethylene oligomerization [4–9], bidentate nickel dihalides bearing P^P [13–15], N^O [16–21], P^N [22–27], N^N [28–37] and organonickel complexes [38,39] have been widely studied for ethylene reactivities. Encouraged by the finding of bis(imino)pyridyl iron and cobalt complexes as highly active catalysts in ethylene reactivity [11,12], special efforts have been paid

to devise new tridentate ligands such as O^N^N [40], N^P^N [41], P^N^N [42,43], and N^N^N [44–49] for their complexes as new catalysts; promisingly some N^N^N tridentate complexes gave good to high activities [50,51] with different models [52] in our group. Especially those catalytic precursors include the iron, cobalt, nickel and other metals, which are dependent of tridentate ligands such as 2-imino-1,10-phenanthroline derivatives (**A**, Scheme 1) [53–58], 2-(2-benzimidazolyl)-6-[1-(arylimino)ethyl] pyridines [59–61], 2-quinoxalinyl-6-iminopyridines [62,63], and 2-methyl-2,4-bis(6-iminopyridin-2-yl)-*1H*-1,5-benzodiazepines [64,65].

Altering its imino-group of model **A** into a N-cyclic group, late transition metal complexes bearing 2-(benzimidazol-2-yl)-1,10-phenanthrolines (**B**, Scheme 1) were synthesized and showed high catalytic activities towards ethylene oligomerization [66,67]. Bianchini group reported that the cobalt complexes bearing 2-thiophen-2-yl-6-iminopyridines showed about 5 times higher active in ethylene oligomerization with longer chain α-olefins than their analogues bearing 2-furanyl-6-iminopyridines (**C**, Scheme 1) [68–70], which indicates the influence of the heteroatoms of ligands. In our extensive research, the ligands could be expectably changed with benzoxazole instead of benzimidazole, and the nickel complexes ligated by benzoxazolyl substituent show higher activity for ethylene dimerization than its benzimidazolyl analogue [60,71,72]. Therefore 2-benzoxazole-1,10-phenanthroline derivatives (**D**, Scheme 1) are synthesized. In addition of alternation of

---
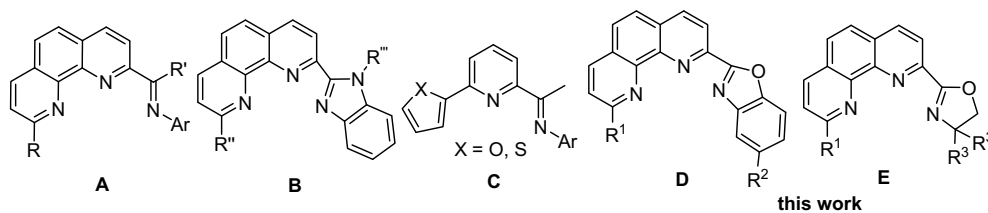
Scheme 1. Ligands for model catalysts.

steric and electronic influences, 2-oxazoline-1,10-phenanthroline derivatives are prepared (**E**, Scheme 1). Their metal (nickel, cobalt or iron) complexes are easily formed and showed higher catalytic activities in ethylene oligomerization than those analogues ligated by 2-(benzimidazol-2-yl)-1,10-phenanthrolines (**B**) [66,67]. Herein the syntheses and characterizations of 2-benzoxazole-1,10-phenanthrolines (**D**), 2-oxazoline-1,10-phenanthrolines (**E**) and their metal (nickel, cobalt or iron) complexes are reported, and the catalytic behaviors of the metal complexes in ethylene oligomerization with different cocatalysts and reaction parameters are investigated and discussed in detail.

2. Results and discussion

2.1. Synthesis and characterization

The synthesis of 2-methyl-1,10-phenanthroline has been performed without any problem on tens gram-scale by the reaction of 8-aminoquinoline with crotonaldehyde according to the literature [73]. 2-Methyl-1,10-phenanthroline was treated with twofold excess of phenyllithium to obtain 2-methyl-9-phenyl-1,10-phenanthroline in 73% yield after the routine workup and separation by column chromatography (Scheme 2).

2-Methyl-1,10-phenanthroline and 2-methyl-9-phenyl-1,10-phenanthroline were oxidized with selenium dioxide to form their corresponding aldehydes, respectively [74,75]. The aldehydes reacted with 2-aminophenol derivatives to afford 2-benzoxazole-

1,10-phenanthrolines (**L1–L4**) in acceptable yields [76]. Formations of benzoxazole and oxazoline differ regarding the role of fused-benzene derivatives, oxazoline-phenanthrolines could not be obtained through direct reaction of its aldehyde with ethanolamines. The alternative synthetic procedure employs the intermediates of methoxyimidates. The aldehydes were converted into corresponding oximes, which could be further dehydrated in acetic anhydride to give the nitriles [74,75]. The methoxyimidates were easily formed in the reaction of nitriles with methanol in the presence of base [77]. After neutralization with acetic acid and subsequent removal of the solvent, condensation of the relevant methoxyimidates with aminoethanol or 2-amino-2-methyl propan-1-ol gave the corresponding oxazoline-phenanthroline derivatives (**L5–L8**) in acceptable yields [78]. All 2-benzoxazole-1,10-phenanthrolines (**L1–L4**) and oxazoline-phenanthrolines (**L5–L8**) are well characterized by IR, ^{1}H, and ^{13}C NMR spectroscopy as well as the elemental analysis. Moreover, the molecular structures of ligand **L2** in the solid state is confirmed by the single-crystal X-ray diffraction.

The routine stoichiometric reactions of the ligands (**L1–L8**) with metal chlorides gave their corresponding complexes in good yields (Scheme 3) [66,67]. The nickel complexes (**Ni1–Ni8**) and cobalt complexes (**Co1–Co8**) in green powders were synthesized by treating the corresponding ligands with an equimolar NiCl$_2$ · 6H$_2$O or CoCl$_2$ in anhydrous ethanol. The iron complexes (**Fe1–Fe8**) in purple powders were readily prepared by mixing the corresponding ligands with one equivalent of FeCl$_2$ · 4H$_2$O in anhydrous ethanol at
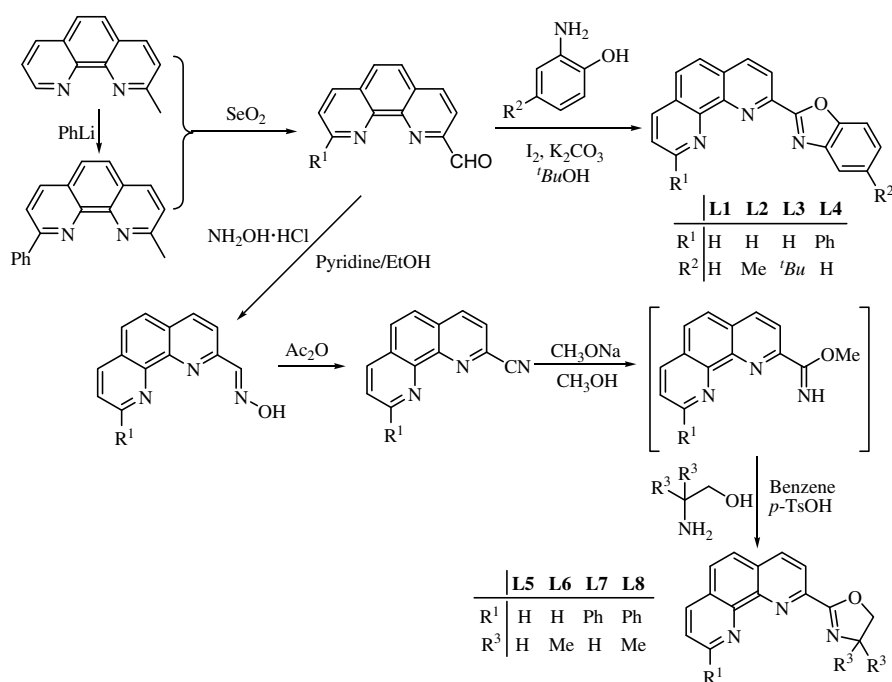
Scheme 2. Synthesis of 2-benzoxazole- or 2-oxazoline-1,10-phenanthrolines (**L1–L8**).
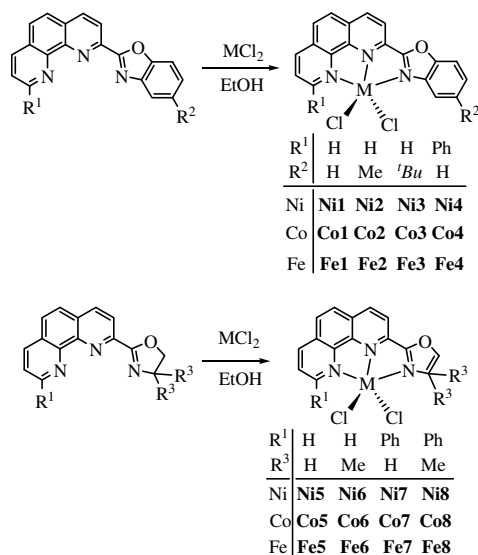
Scheme 3. Synthesis of metal complexes.

room temperature under nitrogen. All resultant complexes precipitated from the reaction solution, filtrated, washed with diethyl ether and dried in vacuum.

All complexes were characterized by IR spectroscopy and elemental analysis. The IR spectra of the complexes show the C=N stretching vibrations of the iron, cobalt, and nickel complexes shifted to lower wave number along with weaker intensities comparing with those of their corresponding ligands, thereby indicates the presence of coordinative interactions between the nitrogen atoms of benzoxazole/oxazoline and imino-groups with the central metal. To confirm their real molecular structures in the solid state, the structures of **Ni3**, **Co1**, **Co3** and **Fe2** are determined by single-crystal X-ray diffraction analysis.

2.2. X-ray crystallographic studies

Crystals of ligand **L2** suitable for X-ray diffraction analysis were grown from dichloromethane/hexane (1:8, v/v) solution at room temperature over several days. Its molecular structure is shown in Fig. 1. The dihedral angle between phenanthrolinyl plane and benzoxazole plane is 9.4°, which is slightly larger than that of (1-methyl-1H-benzimidazol-2-yl)-1,10-phenanthroline (7.6°) [66] and indicates all the non-hydrogen atoms are almost coplanar.
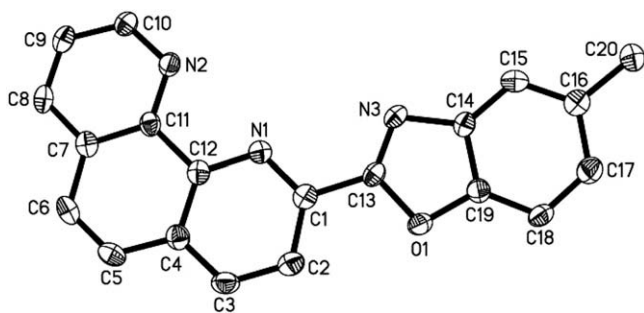
Fig. 1. ORTEP drawing of **L2** with thermal ellipsoids at the 30% probability level. Hydrogen atoms have been omitted for clarity. Selected bond lengths (Å) and angles (deg): C1–C13 1.471(3), C1–N1 1.330(3), C1–C2 1.406(3), C15–C16 1.388(3), C16–C17 1.408(3); C13–C1–C2 119.52(2), N1–C1–C2 123.94(2), N3–C13–O1 115.37(2), C15–C16–C17 119.96(2).

Similarly to the benzoimidazole analogue, the N3–C13 bond length (1.293(3) Å) is relatively longer than the typical imino C=N bond.

Single crystals of complex **Ni3** suitable for X-ray diffraction analysis were grown by slowly laying of diethyl ether into their methanol solutions. The asymmetric unit of complex **Ni3** contains the halves of two independent molecules, as shown in Fig. 2. The two molecules have slightly different bond lengths and bond angels, as shown in Table 1. Complex **Ni3** demonstrates a distorted octahedral coordination geometry of the Ni-center because of the coordination of methanol. One chloride is replaced by one methanol molecule and acts as a counterion. The nickel atom and the mutually *trans*-disposed oxygen atoms are almost in one line [174.40(2)° for (O30–Ni1–O40) in (a) and 174.94(2)° for O30'–Ni1'–O40' in (b)]. The Ni atom deviates slightly out of the coordination plane [0.0094 Å for (a) and 0.0282 Å for (b)]. It is notable that the dihedral angle between phenanthroline plane and benzoxazole plane [0.7° in (a) and 2.7° in (b)] is smaller than those of its benzoimidazole nickel analogues (5.8–7.9°) [66]. In both molecules, the Ni–N(benzoxazole) are longer than the two Ni–N(phenanthroline) bonds, which is different from the benzoimidazole nickel analogues in which the Ni–N(benzoimidazole) are shorter than one of the two Ni–N(phenanthroline) bonds [66].

Single crystals of complexes **Co1**, **Co3** and **Fe2** suitable for X-ray diffraction analysis were grown by diffusing diethyl ether into their methanol solutions. Their structures were depicted in Figs. 3–5, respectively. Their selected bond lengths and angles are listed in Table 2.

In the structure of **Co1** (Fig. 3), the coordination geometry of the cobalt center can be best described as distorted trigonal bipyramidal with the phenanthroline nitrogen atom (N1) and the two chlorines (Cl1 and Cl2) forming the equatorial plane. The cobalt atom slightly deviates by 0.0041 Å from the plane with equatorial angles range between 111.20(1)° and 132.51(1)°. The two axial Co–N bonds subtend an angle of 149.85(2)°. The equatorial plane is nearly perpendicular to the phenanthrolinyl plane, with a dihedral angle of 89.2°. The dihedral angle between phenanthroline plane and benzoxazole plane in **Co1** is 0.9°. The Co1–N1 (phenanthroline) bond is about 0.2281 Å shorter than Co1–N3 (benzoxazole) (2.301(5) Å) bond and 0.1641 Å shorter than Co1–N2 (phenanthroline) (2.237(5) Å) bond respectively.
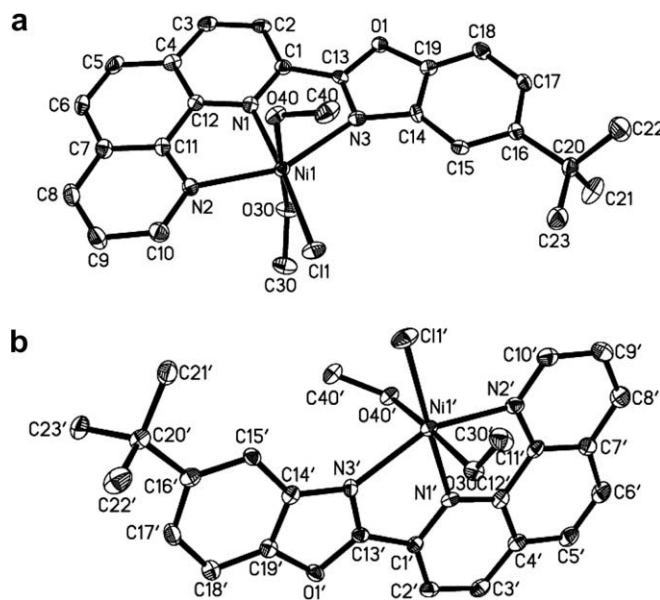
Fig. 2. ORTEP drawing of **Ni3** with thermal ellipsoids at the 30% probability level. Hydrogen atoms have been omitted for clarity.

Table 1
Selected bond lengths (Å) and bond angles (deg) for **Ni3**.

Ni1–N1	2.027(5)	Ni1'–N1'	2.024(4)
Ni1–N2	2.157(4)	Ni1'–N2'	2.157(4)
Ni1–N3	2.215(4)	Ni1'–N3'	2.199(4)
Ni1–Cl1	2.3184(2)	Ni1'–Cl1'	2.3164(2)
C1–C13	1.443(7)	C1'–C13'	1.462(7)
N1–Ni1–N2	77.61(2)	N1'–Ni1'–N2'	77.55(2)
N2–Ni1–N3	153.57(2)	N2'–Ni1'–N3'	153.04(2)
N1–Ni1–N3	75.96(2)	N1'–Ni1'–N3'	75.51(2)
N1–Ni1–Cl1	175.70(1)	N1'–Ni1'–Cl1'	178.06(1)
N2–Ni1–Cl1	98.12(1)	N2'–Ni1'–Cl1'	100.84(1)
N3–Ni1–Cl1	108.31(1)	N3'–Ni1'–Cl1'	106.07(1)

Table 2
Selected bond lengths (Å) and bond angles (deg) for **Co1**, **Co3** and **Fe2**.

	Co1	Co3	Fe2
Bond lengths (Å)			
M–N1	2.073(4)	2.080(4)	2.180(3)
M–N2	2.237(5)	2.199(4)	2.234(3)
M–N3	2.301(5)	2.202(4)	2.289(3)
M–Cl1	2.2529(2)	2.2564(1)	2.3087(1)
M–Cl2	2.2723(2)	2.2962(1)	2.4808(1)
C1–C13	1.472(8)	1.451(7)	1.454(5)
Bond angles (deg)			
N1–M–N2	75.62(2)	75.41(2)	73.75(1)
N2–M–N3	149.85(2)	146.30(1)	144.75(1)
N1–M–N3	74.61(2)	74.19(1)	71.66(1)
N1–M–Cl1	132.51(1)	152.14(1)	169.68(8)
N1–M–Cl2	111.20(1)	96.25(1)	86.58(8)
N2–M–Cl1	97.73(1)	100.10(1)	114.48(8)
N2–M–Cl2	97.94(1)	100.86(1)	90.34(8)
N3–M–Cl1	98.76(1)	99.95(1)	99.26(8)
N3–M–Cl2	97.11(1)	96.58(1)	94.22(8)
Cl1–M–Cl2	116.29(7)	111.55(5)	99.23(5)

Fig. 3. ORTEP drawing of **Co1** with thermal ellipsoids at the 30% probability level. Hydrogen atoms have been omitted for clarity.
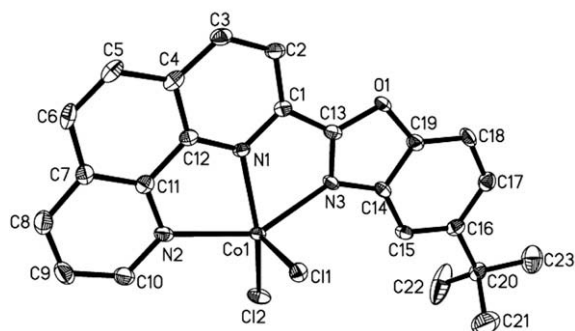
Fig. 4. ORTEP drawing of **Co3** with thermal ellipsoids at the 30% probability level. Hydrogen atoms have been omitted for clarity.
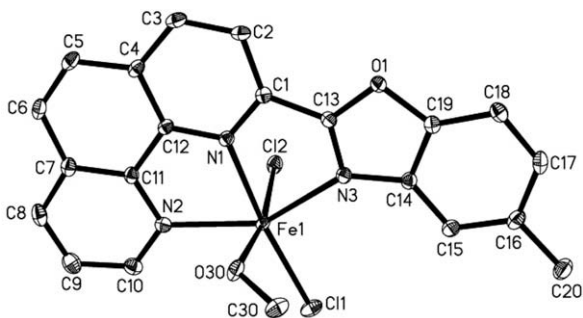
Fig. 5. ORTEP drawing of **Fe2** with thermal ellipsoids at the 30% probability level. Hydrogen atoms have been omitted for clarity.

Unlike complex **Co1**, in the molecular structure of **Co3**, the cobalt atom deviates by 0.3706 Å from the plane formed by N1, N2 and N3; meanwhile the chlorine atom Cl1 is almost in coplanar manner with deviation of 0.3111 Å, and the other chlorine atom Cl2 deviates 2.6595 Å from this plane in the opposite direction. Based on this structural character, the coordination geometry of complex **Co3** can be best described as a distorted square pyramidal with the basal plane composed by N1, N2, N3 and Cl1 (Fig. 4). The similar structure of cobalt complex has been reported [61]. The basal plane is coplanar with the phenanthroline ring (6.9°) and the benzoxazole ring (8.4°).

In the structure of **Fe2** (Fig. 5), the coordination geometry around the iron center can be described as a distorted octahedron because of the coordination of the solvent, which is essentially similar to that of **Ni3** and its benzoimidazole analogue [67]. As expected, the iron center is coordinated to N1, N2 in the phenanthroline ring and N3 in the benzoxazole ring, forming two fused 5-membered rings with acute N–Fe–N angles: 73.75(1)° (N1–Fe1–N2) and 71.66(1)° (N1–Fe1–N3), in which the iron atom lies ca. 0.1882 Å out of the coordinated plane. The benzoxazole plane is nearly coplanar to the phenanthroline plane with a dihedral angle of 4.5°. The bond lengths of Fe–N are significantly different: the Fe1–N1 bond length (2.180(3) Å) is shorter than that of Fe1–N2 (2.234(3) Å) and Fe1–N3 (2.289(3) Å), in which the differences were virtually identical to those seen in the 2,6-bis(imino)pyridyl iron(II) complexes [11,12] and 2-imino-1,10-phenanthrolinyl iron(II) complexes [54].

2.3. Catalytic behavior towards ethylene reactivity

2.3.1. Catalytic behavior of nickel complexes

Complex **Ni1** was typically investigated with various reaction conditions, such as the cocatalysts, molar ratios of cocatalyst to nickel, reaction temperature and ethylene pressure. With cocata-

Table 3
Selection of suitable cocatalyst based on **Ni1**.[a]

Cocat.	Al/Ni	Activity[b]	Oligomer distribution[c] (%)		α-C_4(%)
			$C_4/\sum C$	$C_6/\sum C$	
MAO	1000	0.79	75.8	24.2	50.2
MMAO	1000	0.94	87.4	12.6	52.1
Et$_2$AlCl	200	3.83	90.4	9.6	52.9

[a] Conditions: 5 μmol **Ni1**, 30 mL toluene, 1atm ethylene, 20 °C, 20 min.
[b] 10^5 g mol^{-1}(Ni) h^{-1}.
[c] Determined by GC and $\sum C$ signifies the total amounts of oligomers.

lysts of Et₂AlCl, MAO or MMAO, complex **Ni1** showed moderate activities in ethylene oligomerization for producing butenes and hexenes at 1 atm (Table 3). Cocatalysts significantly affected its catalytic behaviors and Et₂AlCl was found to be more active and selective for α-C4 than MMAO or MAO. Therefore, further catalytic studies were performed with the activation of Et₂AlCl.

The amount of cocatalyst (Et₂AlCl) greatly influenced the catalytic performances. The enhancement of Al/Ni molar ratio from 100 to 200 resulted in an increase of catalytic activity up to 3.83×10^5 g mol^{-1}(Ni) h^{-1} at the Al/Ni ratio of 200. A further increase of the Al/Ni molar ratio showed negative effect from the view of catalytic activity (Entries 1–3, Table 4). Meanwhile, the α-C4 selectivity decreased gradually with the increase of Al/Ni molar ratio. Therefore the Al/Ni molar ratio of 200 is selected in the catalytic systems of other nickel complexes. Notably, compared to its benzimidazole nickel analogue (optimized Al/Ni molar ratio of 300) [66], less amount of Et₂AlCl was used, which may indicates that the benzoxazole substituted nickel complexes are easier to be activated. As the exothermic reaction of oligomerization is concerned, reaction temperature was found to have a remarkable influence on the catalytic activity and the distribution of oligomers obtained. The highest activity was achieved at 20 °C (Entry 2, Table 4), and a slightly lower activity was obtained along with a less amount of butenes (85.6%) produced at lower temperature (0 °C; Entry 4, Table 4). Elevating the reaction temperature from 20 ºC to 60 ºC resulted in a sharp decrease of activity, which may be attributed to the decomposition of the active catalytic sites and lower ethylene solubility at higher temperature. Moreover, higher reaction temperature resulted in an increased proportion of butenes, but a sharp decreased selectivity for 1-butene (Entries 2, 5 and 6, Table 4). The increase of ethylene pressure from 1 to 10 atm ethylene resulted in much higher activities due to an effect of increased ethylene concentration in solution (Entries 2 and 7, Table 4). The better selectivity for 1-butene was also observed at higher pressure, which can be ascribed to the fact that the increased dimerization in turn attenuated the effect of parallel isomerization of 1-butene into 2-butene [25,79,80].

On the base of optimum conditions on **Ni1**, all the nickel complexes **Ni1–Ni8** are investigated at 20 ºC with Al/Ni ratio of 200 and 10 atm ethylene (Entries 7–14, Table 4). It can be observed that ligand environment has considerable effect on the catalytic behaviors, such as activity and α-C4 selectivity. The introduction of a phenyl group on the 9-position of the phenanthroline ring led to a dramatic decrease in catalytic activity and an increase in α-C4 selectivity (Entry 7 vs. Entry 10; Entry 11 vs. Entry 13; Entry 12

vs. Entry 14 in Table 4). Such phenomenon is consistent to the observation that the metal complexes bearing 2-iminophenanthrolines with an additional phenyl group on the 9-position were slightly deactivated and caused by too bulky ligand for ethylene to coordinate to active site [54,58]. Incorporating an electron-donating alkyl group (R² = Me or ᵗBu, R³ = Me) on benzoxazole or oxazoline might push more electrons to the nickel atom, reduce the net charge on the nickel center, and therefore resulted in lower catalytic activity for ethylene oligomerization. This result agrees with the theoretical calculated correlation between the activity and the net charge of the metal center in late-transition metal complexes [81–83] (such as Entries 8 and 9 vs. Entry 7; Entry 12 vs. Entry 11; and Entry 14 vs. Entry 13 in Table 4). Notably, complexes bearing oxazolines display higher catalytic activities with lower selectivities for 1-butene than analogues bearing benzoxazoles (Entry 11 vs. Entry 7; Entry 12 vs. Entry 8; and Entry 13 vs. Entry 10 in Table 4). That could be explained with steric effect of fused benzene ring, moreover, oxazolines provide less electronic donation to metal center than benzoxazoles could.

2.3.2. Catalytic behavior of cobalt complexes

After selection of suitable cocatalyst, MMAO was found the most active. The catalytic activity of cobalt complexes **Co1–Co8** in ethylene oligomerization has been evaluated employing MMAO as cocatalyst under 10 atm of ethylene. Compared to their nickel analogues, all cobalt complexes exhibited lower activities for dimerization and trimerization of ethylene, but with higher selectivities for α-olefins. Similar to their nickel analogues, the additional Ph-group on the 9-position of phenanthroline negatively affects on the cata-

Table 5
Oligomerization of ethylene with **Co1–Co8**/MMAO system.[a]

Entry	Complex	Activity[b]	Oligomer distribution[c](%)		α-C4 (%)
			C4/∑C	C6/∑C	
1	**Co1**	15.1	82.5	17.5	75.6
2	**Co2**	7.88	80.1	19.9	77.3
3	**Co3**	6.32	78.9	21.1	84.3
4	**Co4**	0.57	74.5	25.5	90.9
5	**Co5**	1.92	92.8	7.2	58.2
6	**Co6**	1.58	95.3	4.7	62.1
7	**Co7**	0.77	83.7	16.3	76.4
8	**Co8**	0.68	85.1	14.9	78.1

[a] Conditions: 5 μmol cobalt, 100 mL toluene, 20 ºC, 10 atm ethylene, 20 min, Al/Co = 1000.
[b] 10^5 g mol^{-1}(Co) h^{-1}.
[c] Determined by GC and ∑C signifies the total amounts of oligomers.

Table 4
Ethylene oligomerization by **Ni1–Ni8**/Et₂AlCl system.[a]

Entry	Complex	Al/Ni	T/ºC	P/atm	Activity[b]	Oligomer distribution(%)[c]		α-C4(%)
						C4/∑C	C6/∑C	
1	**Ni1**	100	20	1	1.80	94.8	5.2	55.7
2	**Ni1**	200	20	1	3.83	90.4	9.6	52.9
3	**Ni1**	300	20	1	1.36	89.1	10.9	48.1
4	**Ni1**	200	0	1	1.94	85.6	14.4	65.0
5	**Ni1**	200	40	1	0.53	97.2	2.8	41.3
6	**Ni1**	200	60	1	0.07	98.1	1.9	22.3
7	**Ni1**	200	20	10	25.7	92.0	8.0	63.9
8	**Ni2**	200	20	10	21.9	93.2	6.8	65.7
9	**Ni3**	200	20	10	18.1	91.5	8.5	70.3
10	**Ni4**	200	20	10	10.3	90.1	9.9	84.1
11	**Ni5**	200	20	10	31.1	95.8	4.2	44.2
12	**Ni6**	200	20	10	27.4	97.1	2.9	45.1
13	**Ni7**	200	20	10	14.5	85.1	14.9	60.1
14	**Ni8**	200	20	10	10.9	80.9	19.1	61.3

[a] Conditions: 5 μmol nickel, 20 min, 30 mL toluene for 1 atm ethylene; 100 mL toluene for 10 atm ethylene.
[b] 10^5 g mol^{-1}(Ni) h^{-1}.
[c] Determined by GC and ∑C signifies the total amounts of oligomers.

Table 6
Oligomerization of ethylene with **Fe1**–**Fe8**/MMAO system.[a]

Entry	Complex	Al/Fe	T/°C	P/atm	Activity[b]	Oligomer distribution[c](%)		α-C4(%)
						C4/∑C	C6/∑C	
1	**Fe1**	500	20	1	9.14	89.9	10.1	62.3
2	**Fe1**	800	20	1	18.1	83.5	16.5	60.8
3	**Fe1**	1000	20	1	12.4	86.9	13.1	54.3
4	**Fe1**	800	0	1	7.19	84.5	15.5	65.4
5	**Fe1**	800	30	1	10.5	88.5	11.5	56.7
6	**Fe1**	800	40	1	7.69	90.1	9.9	44.0
7	**Fe1**	800	60	1	2.12	98.3	1.7	25.6
8	**Fe1**	800	20	10	189.3	85.1	14.9	80.3
9	**Fe2**	800	20	10	101.5	83.7	16.3	81.5
10	**Fe3**	800	20	10	91.3	80.1	19.9	83.0
11	**Fe4**	800	20	10	19.7	100		100
12	**Fe5**	800	20	10	25.1	93.5	6.5	61.3
13	**Fe6**	800	20	10	31.7	91.7	8.3	64.7
14	**Fe7**	800	20	10	9.40	95.3	4.7	80.1
15	**Fe8**	800	20	10	15.3	96.0	4.0	83.3

[a] Conditions: 5 μmol iron, 30 mL toluene for 1 atm ethylene; 100 mL toluene for 10 atm ethylene; 20 min.
[b] 10^4 g mol^{-1}(Fe) h^{-1}.
[c] Determined by GC and ∑C signifies the total amounts of oligomers.

lytic activities while causing positive effect on the selectivities for α-olefins (showing with 1-butene in Entry 4 vs. Entry 1; Entry 7 vs. Entry 5; Entry 8 vs. Entry 6, Table 5). A similar tend was observed in complexes bearing ligands with additional alkyl substituents, R^2 (Me or ^tBu, Entries 2 and 3 vs Entry 1, Table 5) or R^3 (Me, Entry 6 vs. Entry 5; Entry 8 vs Entry 7, Table 5). The 2-oxazoline-1,10-phenanthrolinyl cobalt chloride (**Co5**) (Entry 5, Table 5) displayed much lower activity than that of 2-benzoxazole-1,10-phenanthrolinyl cobalt chloride (**Co1**) (Entry 1, Table 5).

2.3.3. Catalytic behavior of iron complexes

After selection of suitable cocatalyst, MMAO was found the most active. Complex **Fe1** was first investigated by employing MMAO as cocatalyst with various ratios at 1 atm of ethylene and then changing reaction temperature. Both cocatalysts activate the iron complex in ethylene oligomerization (Table 6). The amount of cocatalyst has great influence on the catalytic performance. The enhancement of Al/Fe molar ratio from 500 to 800 resulted of increasing catalytic activities in ethylene oligomerization (Entries 1 and 2, Table 6), and the catalytic activity of **Fe1** peaked at 1.81×10^5 g mol^{-1}(Fe) h^{-1} at an Al/Fe molar ratio of 800. Further higher loading of MMAO resulted in decreased activity (Entry 3, Table 6), which could be caused due to unnecessary scavenger and also the isobutyl group from MMAO hindering the insertion reaction of ethylene [84,85]. Similar as its nickel analogue, the α-C4 selectivity of **Fe1** gradually decreased with the increase of the Al/Fe molar ratio.

The reaction temperature affects the catalytic performance. The optimum temperature was 20 °C at 1 atm ethylene (Entry 2, Table 6). The random selectivities of dimer or trimer were observed in changing reaction temperature (Entries 2, 4–7, Table 6). The higher temperature reaction used, the lower selectivity 1-butene observed. A similar influence of temperature on the oligomer distribution produced by iron-based systems has been reported [59].

Based on the above results, the reaction parameters are fixed as 20 °C and an Al/Fe molar ratio of 800. At 10 atm ethylene, the results by all iron complexes in ethylene oligomerization are listed in Table 6 (Entries 8–15). Similarly to the above nickel and cobalt analogues, the phenyl group on the 9-position of phenanthroline ring caused lower activities and higher selectivities for 1-butene (compare Entry 11 vs. Entry 8; Entry 14 vs. Entry 12; Entry 15 vs. Entry 13, Table 6). Moreover, adding other alkyl groups such as R^2 (Me or ^tBu, compare Entries 9 and 10 with Entry 8, Table 6) also led to lower activities and higher selectivities for 1-butene. However, the additional R^3 groups (Me, compare Entry 13 with En-

try 12; Entry 15 with Entry 14, Table 6) resulted in higher activities and selectivities for 1-butene. Both the catalytic activities and selectivities of these iron complexes bearing benzoxazoles (except **Fe4**) were found much higher than those of complexes containing oxazolines, such as examples of **Fe5** with **Fe1** (Entry 12 vs. Entry 8, Table 6) and **Fe7** with **Fe4** (Entry 14 vs. Entry 11, Table 6). All iron complexes exhibited slightly higher activities than those of their cobalt analogues, which commonly observed in tridentate metal (Fe and Co) catalysts in ethylene reactivity [11,12,86].

Compared with 2-benzimidazolylphenanthrolines nickel, iron and cobalt dichloride [66,67], complexes containing a 2-benzoxazole substituent generally showed slightly higher catalytic activity than their 2-benzimidazole analogues. In comparison with benzimidazole analogue, the benzoxazoles which posses stronger electron-withdrawing ability, made more net charge on the nickel center, thus having more positive impact on the catalytic activity than its benzimidazole counterparts. This result is consistent with the computational conclusion related to the relationship between catalytic activity and the net charge of the metal center in late-transition metal complexes [81–83].

3. Conclusions

Metal (nickel, cobalt and iron) complexes ligated by 2-oxazoline- or 2-benzoxadozole-1,10-phenanthrolines have been synthesized, characterized and evaluated as catalyst precursors in ethylene oligomerization. On treatment with Et$_2$AlCl, nickel complexes oligomerized ethylene with high activities (**Ni5**/Et$_2$AlCl: 3.11×10^6 g mol^{-1}(Ni) h^{-1}). Upon activation with MMAO, cobalt and iron complexes showed nice catalytic activities (**Co1**/MMAO: 1.51×10^6 g mol^{-1}(Co) h^{-1}; **Fe1**/MMAO: 1.89×10^6 g mol^{-1}(Fe) h^{-1}). Higher activity and better selectivity for 1-butene could be obtained under higher ethylene pressure and ambient temperature. The variation of oxygen-containing group (benzoxazole or oxazoline) on the 2-position of the phenanthroline ring shows great influence on the catalytic performance of those metal complexes.

4. Experimental

4.1. General considerations

All air- or moisture-sensitive manipulations were carried out under nitrogen using standard Schlenk techniques. Melting points

were determined with a digital electrothermal apparatus without calibration. IR spectra were obtained with a Perkin–Elmer FTIR 2000 spectrophotometer by using KBr disks in the range of 4000–400 cm^{-1}. NMR spectra were recorded with a Bruker DMX-300 or Bruker ARX 400 spectrometer with TMS as the internal standard. Elemental analyses were performed with a Flash EA 1112 microanalyzer. GC was performed with a VARIAN CP-3800 gas chromatograph equipped with a flame ionization detector and a 30-m (0.2 mm i.d., 0.25 μm film thickness) CP-Sil 5 CB column. Toluene was refluxed in the presence of sodium/benzophenone and distilled under nitrogen prior to use. The polymerization-grade ethylene was supplied by Beijing Yansan Petrochemical Co. Et$_2$AlCl (1.90 M) solution in toluene and triethylaluminum (diluted to 2 M in toluene for usage) were purchased from Acros Chemicals, while methylaluminoxane (MAO, 1.46 M in toluene) and modified methylaluminoxane (MMAO, 1.93 M in heptane, 3A) were purchased from Akzo Nobel Corp. All other commercial chemicals were used without further purification.

4.2. Synthesis of ligands (L1–L8)

4.2.1. 2-Methyl-9-phenyl-1,10-phenanthroline

A phenyllithium solution was prepared through the slow addition of bromobenzene (2.31 mL, 22.0 mmol) solution in diethyl ether (20 mL) to two equivalents of lithium (313 mg, 45.0 mmol) in diethyl ether (30 mL) at room temperature under nitrogen. Phenyllithium solution was thereafter added dropwise to a suspension of 2-methyl-1,10-phenanthroline (1.94 g, 10.00 mmol) in toluene (40 mL) at −78 °C and then the mixture was slowly warmed to room temperature and stirred overnight. The reaction was quenched by slow addition of water (100 mL). The brown organic layer was separated and the aqueous layer was extracted several times with CH$_2$Cl$_2$. The organic phases was combined and dried with anhydrous sodium sulfate. After the evaporation of solvent, the residue was purified on a silica column (8/1 petroleum ether/ triethylamine) and the pure product was obtained as ivory white solid in 73% yield (1.97 g). M.p. = 194–196 °C. FT-IR (KBr disc, cm^{-1}): 3059(m), 3042(m), 1651(m), 1608(m, $\upsilon_{C=N}$), 1501(s), 1489(s), 1449(s), 1400(m), 1289(m), 1246(m), 1126(m), 1114(m), 1071(w), 858(s), 744(s), 718(s). ^{1}H NMR (400 MHz, CDCl$_3$): δ = 8.41 (d, J = 7.5 Hz, 2 H, Ph), 8.33 (d, J = 8.4 Hz, 1 H, phen), 8.17 (d, J = 8.2 Hz, 1H, phen), 8.14 (d, J = 8.4 Hz, 1 H, phen), 7.78 (s, 2 H, phen), 7.60–7.48 (m, 4 H, 3 H-Ph, 1 H-phen) ppm. ^{13}C NMR (100 MHz, CDCl$_3$): δ 159.6, 157.1, 145.8, 139.7, 137.0, 136.3, 129.5, 128.8, 128.0, 127.8, 127.1, 126.3, 123.7, 120.2, 26.0 ppm. C$_{19}$H$_{14}$N$_2$ (270.33): calcd. C 84.42, H 5.22, N 10.36. Found C 84.74, H 5.15, N 10.11%.

4.2.2. 1,10-Phenanthroline-2-carbaldehyde

Selenium dioxide (3.42 g, 30.8 mmol) was added to a solution of 2-methyl-1,10-phenanthroline (3.00 g, 15.4 mmol) in dioxane (50 ml). The mixture was heated under reflux for 2 h and then filtered through Celite. Evaporation of the solvent afforded a yellow solid. Some more product was obtained by washing the Celite with CH$_2$Cl$_2$ (3.59 g, 12.6 mmol, 82%). M.p. = 153–155 °C ([lit. 54, [87]]152–154 °C).

4.2.3. 9-Phenyl-1,10-phenanthroline-2-carbaldehyde

In a similar manner to that described for 1,10-phenanthroline-2-carbaldehyde, 9-phenyl-1,10-phenanthroline-2-carbaldehyde was obtained as yellow solid in 79% yield. M.p. = 228–230 °C. FT-IR (KBr disc, cm^{-1}): 3060(m), 2823(s), 1705(s, $\upsilon_{C\equiv N}$), 1614(m, $\upsilon_{C=N}$), 1602(m), 1578(m), 1546(m), 1487(s), 1370(m), 1280(m), 1260(s), 1098(m), 1090(m), 884(s), 797(s), 739(s), 692(s). ^{1}H NMR (400 MHz, CDCl$_3$): δ = 10.56 (s, 1 H, CHO), 8.43–8.36 (m, 4 H, 2 H-phen, 2 H-Ph), 8.30 (d, J = 8.2 Hz, 1 H, phen), 8.20 (d,

J = 8.4 Hz, 1H, phen), 7.97 (d, J = 8.8 Hz, 1 H, phen), 7.86 (d, J = 8.8 Hz, 1 H, phen), 7.59 (t, J = 7.2 Hz, 2 H, Ph), 7.51 (t, J = 7.2 Hz, 1 H, Ph) ppm. ^{13}C NMR (100 MHz, CDCl$_3$): δ = 193.8, 157.7, 151.8, 145.8, 145.6, 138.9, 137.1, 136.8, 131.1, 129.5, 128.9, 128.6, 127.6, 125.5, 120.7, 119.2 ppm. C$_{19}$H$_{12}$N$_2$O (284.31): Calc. C 80.27, H 4.25, N 9.85. Found C 80.54, H 4.15, N 10.11%.

4.2.4. 2-(Benzoxazol-2-yl)-1,10-phenanthroline (L1)

To a solution of 1,10-phenanthroline-2-carbaldehyde (2.08 g, 10 mmol) in *tert*-butyl alcohol (30 ml) was added 2-aminophenol (1.20 g, 11.0 mmol). The mixture was stirred at room temperature under nitrogen atmosphere for 30 min, and then K$_2$CO$_3$ (4.15 g, 30 mmol) and I$_2$ (5.08 g, 20 mmol) were added to the mixture and stirred at 70 °C for 18 h. The reaction was quenched with saturated aqueous Na$_2$SO$_3$ until the iodine color almost disappeared and was extracted with Et$_2$O. The organic layer was washed with brine and dried over Na$_2$SO$_4$. After filtration, the solvent was removed in vacuo. The residual was chromatographed on silica gel (AcOEt) to give 0.68 g of the product as white solid in 23% yield. M.p. = 172–174 °C. FT-IR (KBr disc, cm^{-1}): 3059(m), 1613(m, $\upsilon_{C=N}$), 1586(m), 1549(m), 1501(s), 1489(s), 1449(s), 1400(m), 1289(s), 1246(m), 1126(m), 1113(s), 1065(s), 877(s), 858(s), 764(m), 744(m), 718(s). ^{1}H NMR (400 MHz, CDCl$_3$): δ = 9.32 (dd, J_1 = 1.7 Hz, J_2 = 4.3 Hz, 1 H, phen), 8.74 (d, 1 H, J = 8.3 Hz, phen), 8.45 (d, J = 8.4 Hz, 1 H, phen), 8.30 (dd, J_1 = 1.6 Hz, J_2 = 8.1 Hz, 1 H, phen), 7.92–7.86 (m, 3 H, 1 H-phen, 2 H- benzoxazole), 7.79 (dd, J_1 = 1.4 Hz, J_2 = 6.8 Hz, 1 H, phen), 7.70 (dd, J_1 = 4.4 Hz, J_2 = 8.0 Hz, 1 H, phen), 7.48–7.42 (m, 2 H, benzoxazole), ppm. ^{13}C NMR (100 MHz, CDCl$_3$): δ = 160.9, 150.4, 149.8, 145.1, 145.0, 144.5, 141.0, 136.3, 135.4, 128.6, 128.2, 127.4, 125.5, 125.3, 124.2, 122.7, 121.4, 119.9, 110.8 ppm. C$_{19}$H$_{11}$N$_3$O (297.31): Calc. C 76.76, H 3.73, N 14.13. Found C 76.50, H 4.03, N 14.50%.

4.2.5. 2-(5-Methylbenzoxazol-2-yl)-1,10-phenanthroline (L2)

In a similar manner to that described for **L1**, **L2** was obtained as white solid in 28% yield. M.p. = 198–200 °C FT-IR (KBr disc, cm^{-1}): 3030(m), 1734(m), 1619(m, $\upsilon_{C=N}$), 1585(m), 1549(m), 1502(s), 1482(s), 1443(s), 1418(m), 1402(m), 1352(m), 1311(w), 1263(s), 1192(m), 1108(s), 1080(m), 1069(s), 948(m), 874(s), 853(s), 807(s). ^{1}H NMR (400 MHz, CDCl$_3$): δ = 9.32 (d, J = 4.3 Hz, 1 H, phen), 8.73 (d, 1 H, J = 8.3 Hz, phen), 8.46 (d, J = 8.4 Hz, 1 H, phen), 8.31 (d, J = 8.1 Hz, 1 H, phen), 7.92 (d, J = 8.9 Hz, 1 H, phen), 7.89 (d, J = 8.9 Hz, 1 H, phen), 7.71 (dd, J_1 = 4.3 Hz, J_2 = 8.0 Hz, 1 H, phen), 7.67–7.64 (m, 2 H, benzoxazole), 7.25 (d, J = 6.5 Hz, 1 H, benzoxazole), 2.52 (s, 3 H, CH$_3$) ppm. ^{13}C NMR (100 MHz, CDCl$_3$): δ = 161.6, 150.7, 149.4, 145.8, 145.7, 145.6, 141.9, 136.8, 135.8, 134.5, 129.1, 128.8, 127.9, 127.2, 125.8, 123.1, 122.1, 120.1, 110.1, 21.3 ppm. C$_{20}$H$_{13}$N$_3$O (311.34): Calc. C 77.16, H 4.21, N 13.50. Found C 77.40, H 4.03, N 13.77%.

4.2.6. 2-(5-Tert-butylbenzoxazol-2-yl)-1,10-phenanthroline(L3)

In a similar manner to that described for **L1**, **L3** was obtained as white solid in 47% yield. M.p. = 114–116 °C. FT-IR (KBr disc, cm^{-1}): 3050(m), 2959(s), 2867(m), 1618(m, $\upsilon_{C=N}$), 1586(m), 1544(m), 1503(s), 1481(s), 1442(s), 1419(m), 1269(s), 1108(s), 1080(m), 1064(s), 945(m), 876(m), 856(s), 833(m). ^{1}H NMR (400 MHz, CDCl$_3$): δ = 9.32 (d, J = 4.3 Hz, 1 H, phen), 8.74 (d, 1 H, J = 8.3 Hz, phen), 8.45 (d, J = 8.4 Hz, 1 H, phen), 8.30 (d, J = 8.0 Hz, 1 H, phen), 7.92–7.87 (m, 3 H, 2 H-phen, 1 H-benzoxazole), 7.72-7.67 (m, 2 H, 1 H-phen, 1 H- benzoxazole), 7.51 (d, J = 8.6 Hz, 1 H, benzoxazole), 1.43 (s, 9 H, ^{t}Bu) ppm. ^{13}C NMR (100 MHz, CDCl$_3$): δ = 161.7, 150.8, 149.2, 148.1, 145.9, 145.7, 141.6, 136.9, 135.8, 129.1, 128.8, 127.9, 125.9, 123.9, 123.1, 122.1, 116.6, 110.7, 34.7, 31.5 ppm. C$_{23}$H$_{19}$N$_3$O (353.42): Calc. C 78.16, H 5.42, N 11.89. Found C 78.40, H 5.03, N 11.77%.

4.2.7. 2-(Benzoxazol-2-yl)-9-phenyl-1,10-phenanthroline (**L4**)

In a similar manner to that described for **L1**, **L4** was obtained as white solid in 21% yield using 9-phenyl-1,10-phenanthroline-2-carbaldehyde as the starting material. M.p. = 214–216 °C. FT-IR (KBr disc, cm^{-1}): 3061(m), 3035(m), 2843(m), 1952(m), 1621(m, $\upsilon_{C=N}$), 1603(m), 1587(m), 1579(m), 1546(m), 1487(s), 1450(s), 1422(m), 1368(m), 1245(s), 1115(m), 1102(s), 1063(s), 929(m), 898(m), 886(m), 860(s), 806(m). ^{1}H NMR (400 MHz, CDCl$_3$): δ = 8.75 (d, J = 8.3 Hz, 1 H, phen), 8.50–8.46 (m, 3 H, 2H-Ph, 1 H-phen), 8.37 (d, J = 8.4 Hz, 1 H, phen), 8.21 (d, J = 8.4 Hz, 1 H, phen), 7.94 (d, J = 8.8 Hz, 1 H, phen), 7.88 (m, 2 H, benzoxazole), 7.81 (d, J = 7.4 Hz, 1 H, phen), 7.62 (t, J = 7.3 Hz, 2 H, Ph), 7.53 (t, J = 7.2 Hz, 1 H, Ph), 7.50–7.42 (m, 2 H, benzoxazole) ppm. ^{13}C NMR (100 MHz, CDCl$_3$): δ = 162.1, 157.8, 151.5, 148.8, 147.8, 146.3, 145.9, 145.1, 142.1, 139.3, 137.4, 137.1, 129.8, 129.0, 128.3, 128.0, 125.9, 125.0, 121.6, 120.9, 120.7, 116.3, 111.9 ppm. C$_{25}$H$_{15}$N$_3$O (373.41): Calc. C 80.41, H 4.05, N 11.25. Found C 80.18, H 4.23, N 11.59%.

4.2.8. 1,10-Phenanthroline-2-carboaldoxime

A solution of 1,10-phenanthroline-2-carbaldehyde (0.5 g, 2.40 mmol), hydroxylamine hydrochloride (0.5 g, 7.20 mmol) and pyridine (1 ml) in ethanol (30 ml) was heated under reflux for 2 h. The resulting green precipitate was recrystallized from ethanol to give the product in 92% yield. M.p. = 224–226 °C. FT-IR (KBr disc, cm^{-1}): 3600–2800(s), 1615(m, $\upsilon_{C=N}$), 1596(s), 1531(s), 1461(s), 1402(s), 1349(m), 1288(s), 1228(s), 1190(s), 1139(s), 1100(m), 990(s), 961(m), 941(s), 884(m), 867(s), 825(s), 818(m), 729(s). ^{1}H NMR (400 MHz, DMSO): δ = 12.0 (s, OH), 8.65–8.61 (m, 2 H, phen), 8.55 (s, 1 H, C*H*=NOH), 8.46–8.42 (m, 3 H, phen), 8.24 (d, J = 8.5 Hz, 1 H, phen), 8.08–8.06 (m, 2 H, Ph), 7.63–7.56 (m, 3 H, Ph) ppm. ^{13}C NMR (100 MHz, DMSO): δ = 153.4, 148.9, 144.5, 140.2, 138.5, 130.1, 129.7, 129.1, 127.9, 126.8, 125.4, 122.0 ppm. C$_{13}$H$_9$N$_3$O (223.23): Calc. C 69.95, H 4.06, N 18.82. Found C 69.78, H 4.23, N 18.59%.

4.2.9. 9-Phenyl-1,10-phenanthroline-2-carboaldoxime

In a similar manner to that described for 1,10-phenanthroline-2-carboaldoxime, 9-phenyl-1,10-phenanthroline-2-carboaldoxime was obtained as green solid in 87% yield. M.p. = 360–362 °C. FT-IR (KBr disc, cm^{-1}): 3600–2800(s), 1895(m), 1628(m, $\upsilon_{C=N}$), 1577(s), 1557(s), 1531(s), 1507(m), 1479(s), 1442(m), 1418(m), 1332(m), 1308(s), 1193(s), 1161(s), 1013(s), 999(s), 883(m), 868(s), 856(s), 773(m), 765(m), 753(m), 729(s), 688(s), 672(m). ^{1}H NMR (400 MHz, DMSO): δ = 12.0 (s, OH), 8.65–8.61 (m, 2 H, phen), 8.55 (s, I H, C*H*=NOH), 8.46–8.42 (m, 3 H, phen), 8.24 (d, J = 8.5 Hz, 1 H, phen), 8.17 (d, J = 8.7 Hz, 1 H, Ph), 8.05 (d, J = 8.8 Hz, 1 H, Ph) 7.63–7.52 (m, 3 H, Ph) ppm. ^{13}C NMR (100 MHz, DMSO): δ = 152.3, 149.0, 144.5, 141.0, 138.7, 137.3, 130.5, 129.9, 129.4, 128.7, 127.0, 126.5, 125.4, 122.3, 119.6 ppm. C$_{19}$H$_{13}$N$_3$O (299.33): Calc. C 76.24, H 4.38, N 14.04. Found C 76.58, H 4.33, N 13.79%.

4.2.10. 1,10-phenanthroline-2-carbonitrile

A solution of 1,10-phenanthroline-2-carboaldoxime (0.5 g, 2.24 mmol) in acetic anhydride (10 ml) was heated under reflux for 2 h. After dilution with water (20 mL) and neutralization by NaHCO$_3$, the aqueous phase was extracted by CH$_2$Cl$_2$ and purified by silica gel column (1/2 EtOAc/Petroleum ether) to give the product as white solid in 54% yield. M.p. = 231–233 °C. ([lit. 54, [88]] 233–234 °C].

4.2.11. 9-Phenyl-1,10-phenanthroline-2-carbonitrile

In a similar manner to that described for 1,10-phenanthroline-2-carbonitrile, the product was obtained as yellow solid in 48% yield. M.p. = 264–266 °C. FT-IR (KBr disc, cm^{-1}): 3054(m), 2233(m), 1960(w), 1616(m, $\upsilon_{C=N}$), 1601(m), 1576(m), 1542(m), 1504(m), 1485(s), 1420(m), 1404(m), 1364(m), 1299(m), 1280(m), 1206(m), 1148(m), 1100(m), 1023(m), 911(m), 863(s). ^{1}H NMR (400 MHz, CDCl$_3$): δ = 8.40–8.35 (m, 4 H, 2 H-phen, 2 H-Ph), 8.21 (d, J = 8.4 Hz, 1 H, phen), 8.01–7.96 (m, 2 H, phen), 7.82 (d, J = 8.8 Hz, 1 H, phen), 7.59 (t, J = 7.4 Hz, 2 H, Ph), 7.51 (t, J = 7.1 Hz, 1 H, Ph) ppm. ^{13}C NMR (100 MHz, CDCl$_3$): δ = 158.3, 146.9, 145.3, 139.0, 137.4, 137.2, 133.4, 130.3, 129.8, 129.1, 128.1, 128.0, 126.1, 125.5, 121.5, 118.0 ppm. C$_{19}$H$_{11}$N$_3$ (281.31): Calc. C 81.12, H 3.94, N 14.94. Found C 81.48, H 3.63, N 14.89%.

4.2.12. 2-(4,5-Dihydrooxazol-2-yl)-1,10-phenanthroline (**L5**)

1,10-Phenanthroline-2-carbonitrile was converted into the corresponding methyl carboxyimidate following a reported method [77]. A solution of methyl carboxyimidate (1.90 g, 8 mmol) in anhydrous benzene containing the appropriate aminoalcohol (488 mg, 8 mmol) and a few milligrams of *p*-toluenesulfonic acid was slowly distilled under nitrogen atmosphere until all the substrate was reacted (1–2 h). The solvent was removed and the residual was purified through silica (acetone as eluent) to give 0.58 g of the product as white solid in 29% yield. M.p. = 88–90 °C. FT-IR (KBr disc, cm^{-1}): 3058(m), 2933(m), 2879(w), 1652(m, $\upsilon_{C=N}$), 1617(m), 1559(m), 1508(m), 1493(m), 1401(s), 1356(m), 1260(w), 1151(m), 1136(s), 1114(m), 1081(s), 949(s), 857(s), 719(s), 704(s). ^{1}H NMR (400 MHz, CDCl$_3$): δ = 9.13 (d, 1 H, J = 8.0 Hz, phen), 8.24 (s, 2 H, phen), 8.17 (d, 1 H, J = 8.0 Hz, phen), 7.73–7.71 (m, 2 H, phen), 7.59–7.56 (m, 1 H, phen), 4.57 (t, J = 9.5 Hz, 2 H, CH$_2$), 4.15 (t, J = 9.7 Hz, 2 H, CH$_2$). ^{13}C NMR (100 MHz, CDCl$_3$): δ = 164.4, 150.5, 146.2, 145.9, 145.6, 136.8, 136.3, 129.5, 129.0, 128.2, 126.2, 123.5, 122.7, 80.0, 68.5, 55.1. C$_{15}$H$_{11}$N$_3$O (249.27): Calc. C 72.28, H 4.45, N 16.86. Found C 72.18, H 4.33, N 17.19%.

4.2.13. 2-(4,5-Dihydro-4,4-dimethyloxazol-2-yl)-1,10-phenanthroline (**L6**)

In a similar manner to that described for **L5**, the product **L6** was obtained as white solid in 31% yield. M.p. = 78–80 °C FT-IR (KBr disc, cm^{-1}): 3057(m), 2967(m), 2931(m), 2900(m), 2867(w), 1690(m), 1645(m, $\upsilon_{C=N}$), 1618(m), 1586(m), 1559(m), 1506(m), 1492(s), 1464(m), 1400(s), 1369(m), 1357(m), 1308(s), 1200(m), 1175(m), 1128(s), 1077(s), 963(s), 861(s), 712(s). ^{1}H NMR (400 MHz, CDCl$_3$): δ = 9.22 (d, 1 H, J = 4.4 Hz, phen), 8.40 (d, 1 H, J = 8.4 Hz, phen), 8.31 (d, 1 H, J = 8.3 Hz, phen), 8.26 (d, 1H, J = 8.1Hz, phen), 7.85 (d, 1 H, J = 8.8 Hz, phen), 7.81 (d, 1 H, J = 8.8 Hz, phen), 7.66 (dd, 1H, J = 4.4, 8.0 Hz, phen), 4.32 (s, 2H, CH$_2$), 1.47 (s, 6H, CH$_3$) ppm. ^{13}C NMR (100 MHz, CDCl$_3$): δ = 161.8, 150.5, 146.5, 146.0, 145.6, 136.8, 136.4, 129.5, 129.0, 128.1, 126.2, 123.5, 122.8, 80.0, 68.2, 28.6 ppm. C$_{17}$H$_{15}$N$_3$O (277.32): Calc. C 73.63, H 5.45, N 15.15. Found C 73.28, H 5.53, N 15.49%.

4.2.14. 2-(4,5-Dihydrooxazol-2-yl)-9-phenyl-1,10-phenanthroline (**L7**)

In a similar manner to that described for **L5**, the product **L7** was obtained as white solid in 34% yield. M.p. = 108–110 °C FT-IR (KBr disc, cm^{-1}): 2924(m), 1632(m, $\upsilon_{C=N}$), 1615(m), 1605(m), 1585(m), 1543(m), 1498(s), 1484(m), 1371(m), 1356(m), 1307(s), 1276(m), 1114(s), 1098(m), 1070(m), 949(s), 857(s), 772(s), 733(s), 698(s). ^{1}H NMR (400 MHz, CDCl$_3$): δ = 8.41–8.31 (m, 5 H), 8.14 (d, 1 H, J = 8.4 Hz, Phen), 7.88 (d, 1 H, J = 8.7 Hz, phen), 7.80 (d, 1 H, J = 8.2 Hz, phen), 7.56 (t, 2 H, J = 7.3 Hz, Ph), 7.48 (t, 1 H, J = 7.2 Hz, Ph). ^{13}C NMR (100 MHz, CDCl$_3$): δ = 164.7, 158.0, 146.5, 146.0, 145.8, 139.3, 137.1, 137.0, 130.1, 129.7, 128.9, 128.2, 128.0, 125.8, 122.7, 121.1, 68.4, 55.3. C$_{21}$H$_{15}$N$_3$O (325.36): Calc. C 77.52, H 4.65, N 12.91. Found C 77.18, H 5.03, N 12.59%.

4.2.15. 2-(4,5-Dihydro-4,4-dimethyloxazol-2-yl)-9-phenyl-1,10-phenanthroline (L8)

In a similar manner to that described for **L5**, the product **L8** was obtained as white solid in 27% yield. M.p. = 100–102 °C FT-IR (KBr disc, cm^{-1}): 3057(m), 2965(m), 2927(m), 1637(m, $\upsilon_{C=N}$), 1618(m), 1605(m), 1588(m), 1506(m), 1499(m), 1487(m), 1425(m), 1364(m), 1304(s), 1188(m), 1131(s), 1110(m), 1069(m), 967(s), 863(s), 770(s), 723(s), 696(s). ^{1}H NMR (400 MHz, CDCl$_3$): δ = 8.45 (d, 1 H, J = 8.3 Hz, phen), 8.40 (d, 2 H, J = 7.5 Hz, Ph), 8.42 (d, 2 H, J = 8.2 Hz, phen), 7.89 (d, 1 H, J = 8.7 Hz, phen), 7.81 (d, 1 H, J = 8.7 Hz, phen), 7.56 (t, 2 H, J = 7.1 Hz, Ph), 7.48 (t, 1 H, J = 7.1 Hz, Ph), 4.35 (s, 2 H), 1.48 (s, 6 H, CH$_3$). ^{13}C NMR (100 MHz, CDCl$_3$): δ = 162.1, 157.8, 146.9, 146.0, 145.8, 139.3, 137.0, 136.8, 130.0, 129.6, 128.9, 128.1, 128.0, 127.9, 125.8, 122.9, 120.9, 79.8, 68.2, 28.7. C$_{23}$H$_{19}$N$_3$O (353.42): Calc. C 78.16, H 5.42, N 11.89. Found C 78.48, H 5.13, N 11.69%.

4.3. Synthesis of nickel complexes Ni1–Ni8 and cobalt complexes Co1–Co8

4.3.1. General considerations

To a solution of 0.20 mmol of NiCl$_2$·6H$_2$O or CoCl$_2$ in 10 mL of anhydrous ethanol was added 0.20 mmol of ligand (suspended in 10 mL of ethanol). The suspension was heated for 30 min at 80 °C, and afterward the solution was stirred overnight at room temperature. Diethyl ether (30 mL) was added to precipitate the product, which was subsequently collected with filtration, washed with diethyl ether and dried in vacuum. All the nickel or cobalt complexes were obtained as green powders in high yields.

Nickel complexes **(Ni1–Ni8)**. **Ni1**: Green powder in 89% yield. IR (KBr disk, cm^{-1}): 3055(m), 1625(m), 1605(m), 1585(m, $\upsilon_{C=N}$), 1549(m), 1451(s), 1436(s), 1419(s), 1366(m), 1347(m), 1304(m), 1150(m), 885(s), 865(s), 810(s), 766(m), 754(m), 711(s). Anal. Calc. for C$_{19}$H$_{11}$N$_3$NiCl$_2$O(426.91): C, 53.45; H, 2.60; N, 9.84. Found: C, 53.66; H, 2.55; N, 9.48%. **Ni2**: Green powder in 79% yield. IR (KBr disk, cm^{-1}): 3060(m), 1625(m), 1582(m, $\upsilon_{C=N}$), 1546(m), 1500(m), 1457(s), 1417(s), 1364(m), 1348(m), 1167(m), 1136(m), 887(s), 862(s), 814(s), 711(s). Anal. Calc. for C$_{20}$H$_{13}$N$_3$NiCl$_2$O (440.94): C, 54.48; H, 2.97; N, 9.53. Found: C, 54.13; H, 3.19; N, 9.69%. **Ni3**: Green powder in 84% yield. IR (KBr disk, cm^{-1}): 3061(m), 2948(m), 1624(m), 1582(m, $\upsilon_{C=N}$), 1523(m), 1497(m), 1480(m), 1457(s), 1416(s), 1365(m), 1350(m), 1159(m), 888(s), 868(s), 823(s), 784(s), 760(m), 713(s). Anal. Calc. for C$_{23}$H$_{19}$N$_3$NiCl$_2$O (483.02): C, 57.19; H, 3.96; N, 8.70. Found: C, 56.81; H, 3.70; N, 8.99%. **Ni4**: Green powder in 88% yield. IR (KBr disk, cm^{-1}): 3062(m), 2970(m), 1636(m), 1606(m), 1576(m, $\upsilon_{C=N}$), 1499(m), 1462(s), 1418(s), 1391(m), 1378(m), 1332(m), 1304(m), 1201(m), 1162(m), 1145(m), 937(s), 866(s), 708(s). Anal. Calc. for C$_{25}$H$_{15}$N$_3$NiCl$_2$O (503.01): C, 59.69; H, 3.01; N, 8.35. Found: C, 59.49; H, 3.32; N, 8.27%. **Ni5**: Green powder in 85% yield. IR (KBr disk, cm^{-1}): 3034(m), 2929(m), 1641(m), 1614(m, $\upsilon_{C=N}$), 1605(m), 1583(m), 1574(m), 1498(m), 1422(s), 1390(m), 1276(m), 1170(m), 1141(m), 869(s), 698(s). Anal. Calc. for C$_{15}$H$_{11}$N$_3$NiCl$_2$O (378.87): C, 47.55; H, 2.93; N, 11.09. Found: C, 47.52; H, 3.15; N, 10.88%. **Ni6**: Green powder in 77% yield. IR (KBr disk, cm^{-1}): 2970(m), 1644(m), 1607(m, $\upsilon_{C=N}$), 1463(m), 1418(s), 1201(m), 1161(m), 937(s), 866(s), 707(s). Anal. Calc. for C$_{17}$H$_{15}$N$_3$NiCl$_2$O (406.92): C, 50.18; H, 3.72; N, 10.33. Found: C, 50.22; H, 3.51; N, 10.48%. **Ni7**: Green powder in 79% yield. IR (KBr disk, cm^{-1}): 1643(m), 1618(m, $\upsilon_{C=N}$), 1562(m), 1491(m), 1460(m), 1396(m), 1280(m), 1176(m), 1059(m), 1022(m), 872(s), 755(s), 720(s). Anal. Calc. for C$_{21}$H$_{15}$N$_3$NiCl$_2$O (454.96): C, 55.44; H, 3.32; N, 9.24. Found: C, 55.22; H, 3.59; N, 9.48%. **Ni8**: Green powder in 86% yield. IR (KBr disk, cm^{-1}): 2970(m), 1617(m, $\upsilon_{C=N}$), 1503(m), 1461(m), 1400(m), 1316(m), 1180(m), 942(m), 879(s), 784(s), 757(s), 709(s), 663(s). Anal. Calc. for C$_{23}$H$_{19}$N$_3$NiCl$_2$O

(483.02): C, 57.19; H, 3.96; N, 8.70. Found: C, 57.52; H, 3.60; N, 8.40%.

Cobalt complexes **(Co1–Co8)**. **Co1**: Green powder in 89% yield. IR (KBr disk, cm^{-1}): 3060(m), 1624(m), 1602(m), 1578(m, $\upsilon_{C=N}$), 1550(m), 1500(m), 1413(s), 1154(s), 861(s), 768(m), 750(s), 710(s). Anal. Calc. for C$_{19}$H$_{11}$N$_3$CoCl$_2$O (427.15): C, 53.42; H, 2.60; N, 9.84. Found: C, 53.66; H, 2.55; N, 9.48%. **Co2**: Green powder in 79% yield. IR (KBr disk, cm^{-1}): 3056(m), 1625(m), 1580(m, $\upsilon_{C=N}$), 1549(m), 1500(m), 1412(s), 1163(s), 885(m), 862(s), 808(s), 748(s), 710(s). Anal. Calc. for C$_{20}$H$_{13}$N$_3$CoCl$_2$O (441.18): C, 54.45; H, 2.97; N, 9.52. Found: C, 54.80; H, 3.19; N, 9.19. **Co3**: Green powder in 80% yield. IR (KBr disk, cm^{-1}): 3059(m), 2964(m), 1625(m), 1578(m, $\upsilon_{C=N}$)), 1546(m), 1497(m), 1411(s), 1361(m), 1156(s), 887(m), 872(s), 821(s), 712(s). Anal. Calc. for C$_{23}$H$_{19}$N$_3$CoCl$_2$O(483.26): C, 57.16; H, 3.96; N, 8.70. Found: C, 57.51; H, 3.60; N, 8.31%. **Co4**: Green powder in 84% yield. IR (KBr disk, cm^{-1}): 3055(m), 1625(m), 1582(m, $\upsilon_{C=N}$), 1538(m), 1507(m), 1487(m), 1456(m), 1382(m), 1364(m), 1159(s), 869(s). Anal. Calc. for C$_{25}$H$_{15}$N$_3$CoCl$_2$O (503.25): C, 59.67; H, 3.00; N, 8.35. Found: C, 59.59; H, 3.32; N, 8.27%. **Co5**: Green powder in 77% yield. IR (KBr disk, cm^{-1}): 3057(m), 1621(m, $\upsilon_{C=N}$), 1583(m), 1482(m), 1449(m), 1337(m), 1155(s), 866(s), 752(s). Anal. Calc. for C$_{15}$H$_{11}$N$_3$CoCl$_2$O (379.11): C, 47.52; H, 2.92; N, 11.08. Found: C, 47.18; H, 3.25; N, 11.38%. **Co6**: Green powder in 73% yield. IR (KBr disk, cm^{-1}): 3042(m), 1641(m), 1616(m, $\upsilon_{C=N}$), 1604(m), 1514(m), 1462(m), 1414(m), 1374(m), 1338(m), 1302(m), 1161(s), 932(s), 864(s), 707(s). Anal. Calc. for C$_{17}$H$_{15}$N$_3$CoCl$_2$O (407.16): C, 50.15; H, 3.71; N, 10.32. Found: C, 50.00; H, 3.91; N, 10.68%. **Co7**: Green powder in 70% yield. IR (KBr disk, cm^{-1}): 3050(m), 1641(m), 1618(m, $\upsilon_{C=N}$), 1607(m, $\upsilon_{C=N}$), 1563(m), 1490(m), 1395(m), 1279(m), 1173(m), 866(s), 704(s). Anal. Calc. for C$_{21}$H$_{15}$N$_3$CoCl$_2$O (455.2): C, 55.41; H, 3.32; N, 9.23. Found: C, 55.20; H, 3.51; N, 9.58. **Co8**: Green powder in 72% yield. IR (KBr disk, cm^{-1}): 3050(m), 1627(m, $\upsilon_{C=N}$), 1585(m), 1475(m), 1450(m), 1388(m), 1163(s), 865(s), 699(s). Anal. Calc. for C$_{23}$H$_{19}$N$_3$CoCl$_2$O (483.26): C, 57.16; H, 3.96; N, 8.70. Found: C, 57.20; H, 3.81; N, 9.0%8.

4.4. Synthesis of iron complexes Fe1–Fe8

4.4.1. General considerations

The ligand (0.20 mmol) and 1 equiv. of FeCl$_2$ · 4H$_2$O (0.20 mmol) were placed in a Schlenk tube, which was then purged three times with nitrogen and then charged with 10 mL of ethanol. The reaction mixture was then stirred at room temperature for 9 h. The resulting precipitate was filtered, washed with diethyl ether and dried in vacuo to give the corresponding iron complex. All the iron(II) complexes were isolated as purple powders in high yields.

Iron complexes **(Fe1–Fe8)**. **Fe1**: Purple powder in 81% yield. IR (KBr disk, cm^{-1}): 3052(m), 1622(m), 1580(m, $\upsilon_{C=N}$), 1547(m), 1499(m), 1411(m), 1362(m), 1144(s), 1042(s), 883(m), 859(s), 791(s), 749(s), 711(s). Anal. Calc. for C$_{19}$H$_{11}$N$_3$FeCl$_2$O (424.06): C, 53.81; H, 2.61; N, 9.91. Found: C, 53.59; H, 2.42; N, 10.25%. **Fe2**: Purple powder in 73% yield. IR (KBr disk, cm^{-1}): 3049(m), 1623(m), 1585(m, $\upsilon_{C=N}$), 1484(m), 857(s), 741(s). Anal. Calc. for C$_{20}$H$_{13}$N$_3$FeCl$_2$O (438.09): C, 54.83; H, 2.99; N, 9.59. Found: C, 54.61; H, 2.64; N, 9.87%. **Fe3**: Purple powder in 66% yield. IR (KBr disk, cm^{-1}): 3052(m), 1623(m), 1579(m, $\upsilon_{C=N}$), 1549(m), 1500(m), 1479(m), 1410(m), 1360(m), 1155(s), 1141(s), 1120(s), 1038(s), 938(s), 886(m), 860(s), 835(s), 817(s), 753(s), 713(s). Anal. Calc. for C$_{23}$H$_{19}$N$_3$FeCl$_2$O (480.17): C, 57.53; H, 3.99; N, 8.75. Found: C, 57.55; H, 3.71; N, 8.91%. **Fe4**: Purple powder in 71% yield. IR (KBr disk, cm^{-1}): 3057(m), 1624(m), 1583(m, $\upsilon_{C=N}$), 1540(m), 1455(m), 1366(m), 1314(m), 1149(s), 864(s). Anal. Calc. for C$_{25}$H$_{15}$N$_3$FeCl$_2$O (500.16): C, 60.03; H, 3.02; N, 8.40. Found: C,

Table 7
Crystal data and structure refinement for **L2**, **Ni3**, **Co1**, **Co3** and **Fe2**.

	L2	Ni3	Co1	Co3	Fe2
Formula	$C_{20}H_{13}N_3O \cdot CH_2Cl_2$	$C_{23}H_{19}Cl_2NiN_3O \cdot 5/2CH_3OH$	$C_{19}H_{11}Cl_2CoN_3O$	$C_{23}H_{19}Cl_2CoN_3O$	$C_{20}H_{13}Cl_2FeN_3O \cdot CH_3OH$
fw	396.26	563.13	427.14	483.24	470.13
Temperature(K)	173(2)	173(2)	293(2)	173(2)	173(2)
Wavelength(Å)	0.71073	0.71073	0.71073	0.71069	0.71073
Cryst syst	Orthorhombic	Monoclinic	Monoclinic	Monoclinic	Triclinic
Space group	$Pbca$	$P2(1)/c$	$P2(1)/n$	$P2(1)/c$	$P1$
a(Å)	7.1956(1)	14.530(3)	7.8120(2)	12.494(3)	6.7650(1)
b(Å)	14.399(3)	20.637(4)	13.132(3)	10.200(2)	10.756(2)
c(Å)	35.157(7)	17.546(4)	16.798(3)	16.825(3)	14.665(3)
α(deg)	90	90	90	90	107.28(3)
β(deg)	90	100.57(3)	96.04(3)	90.73(3)	95.76(3)
γ(deg)	90	90	90	90	104.11(3)
Volume(Å^3)	3642.7(1)	5172.1(2)	1713.7(6)	2143.9(7)	970.8(3)
Z	8	8	4	4	2
D_{calc}(g m^{-3})	1.445	1.446	1.656	1.497	1.608
μ (mm^{-1})	0.373	0.991	1.326	1.070	1.076
$F(000)$	1632	2344	860	988	480
Crystal size (mm)	$0.25 \times 0.15 \times 0.08$	$0.35 \times 0.25 \times 0.15$	$0.35 \times 0.30 \times 0.20$	$0.27 \times 0.20 \times 0.05$	$0.58 \times 0.35 \times 0.07$
θ range (deg)	1.16–27.33	1.54–25.00	1.97–25.01	2.33–25.50	1.48–27.48
Limiting indicates	$-9 \leqslant h \leqslant 9$	$-16 \leqslant h \leqslant 17$	$-9 \leqslant h \leqslant 9$	$-15 \leqslant h \leqslant 15$	$-8 \leqslant h \leqslant 8$
	$-18 \leqslant k \leqslant 18$	$-24 \leqslant k \leqslant 24$	$-15 \leqslant k \leqslant 15$	$-12 \leqslant k \leqslant 12$	$-13 \leqslant k \leqslant 13$
	$-45 \leqslant l \leqslant 45$	$-20 \leqslant l \leqslant 20$	$-19 \leqslant l \leqslant 19$	$-20 \leqslant l \leqslant 20$	$-19 \leqslant l \leqslant 18$
No. of reflections collected	7668	29216	5808	7639	7875
No. of unique reflections	4113	9114	3018	3990	4426
R_{int}	0.0173	0.0824	0.0509	0.0556	0.0318
Completeness to θ (%)	99.9% (θ = 27.33 º)	100.0 (θ = 25.00 º)	100.0 (θ = 25.01 º)	99.9 (θ = 25.50º)	99.6 (θ = 27.48º)
Absorp corr	Empirical	Empirical	Empirical	Empirical	Empirical
no. of params	245	643	235	300	266
Goodness-of-fit on F^2	1.057	1.332	1.196	1.216	1.290
Final R indices ($I > 2\sigma(I)$)	$R_1 = 0.0474$	$R_1 = 0.0908$	$R_1 = 0.0733$	$R_1 = 0.0746$	$R_1 = 0.0565$
	$wR_2 = 0.1160$	$wR_2 = 0.1465$	$wR_2 = 0.1278$	$wR_2 = 0.1278$	$wR_2 = 0.1244$
R indices (all data)	$R_1 = 0.0726$	$R_1 = 0.1174,$	$R_1 = 0.1179$	$R_1 = 0.1049$	$R_1 = 0.0751$
	$wR_2 = 0.1253$	$wR_2 = 0.1554$	$wR_2 = 0.1488$	$wR_2 = 0.1371$	$wR_2 = 0.1374$
Largest difference peak, hole(e Å^{-3})	0.503, −0.586	0.653, −0.552	0.587, −0.483	0.471, −0.530	0.665, −0.546

60.29; H, 3.15; N, 8.29%. **Fe5**: Purple powder in 69% yield. IR (KBr disk, cm^{-1}): 3052(m), 1639(m), 1606(m, $\upsilon_{C=N}$), 1577(m), 1510(m), 1440(m), 1299(m), 1061(s), 867(s), 708(s). Anal. Calc. for $C_{15}H_{11}N_3FeCl_2O$ (376.02): C, 47.91; H, 2.95; N, 11.18. Found: C, 47.72; H, 2.59; N, 11.52%. **Fe6**: Purple powder in 71% yield. IR (KBr disk, cm^{-1}): 3058(m), 2974(m), 1643(m), 1606(m, $\upsilon_{C=N}$), 1578(m), 1515(m), 1421(m), 1334(m), 1304(m), 1168(s), 1046(s), 943(s), 869(s), 837(s), 708(s). Anal. Calc. for $C_{17}H_{15}N_3FeCl_2O$(404.07): C, 50.53; H, 3.74; N, 10.40. Found: C, 50.66; H, 3.49; N, 10.61%. **Fe7**: purple powder in 74% yield. IR (KBr disk, cm^{-1}): 3056(m), 2961(m), 1626(m, $\upsilon_{C=N}$), 1580(m), 1479(m), 1460(m), 1385(m), 1162(s), 864(s). Anal. Calc. for $C_{21}H_{15}N_3FeCl_2O$(452.11): C, 55.79; H, 3.34; N, 9.29. Found: C, 55.66; H, 3.49; N, 9.61%. **Fe8**: purple powder in 70% yield. IR (KBr disk, cm^{-1}): 3053(m), 1630(m, $V_{C=N}$), 1583(m), 1479(m), 1452(m), 1384(m), 1165(s), 868(s), 697(s). Anal. Calc. for $C_{23}H_{19}N_3FeCl_2O$(480.17): C, 57.53; H, 3.99; N, 8.75. Found: C, 57.76; H, 3.79; N, 8.61%.

4.5. General procedure for ethylene oligomerization

A 250-mL stainless steel autoclave equipped with a mechanical stirrer and a temperature controller was heated in vacuo at 80 ℃ for 2 h. It was cooled to the required reaction temperature under ethylene, and charged with toluene, the desired amount of cocatalyst, and toluene solution of catalytic precursor; the total volume was 100 mL. The reactor was sealed and pressurized to the desired ethylene pressure, and the ethylene pressure was maintained with feeding of ethylene. After the reaction was carried out for the required period, the pressure was released. A small amount of the reaction solution was collected, the reaction in this small sample was terminated by the addition of 5% aqueous hydrogen chloride, and the organic layer was analyzed by gas chromatography (GC)

for determining the composition and mass distribution of oligomers obtained.

4.6. X-ray crystallographic studies

Single-crystal X-ray diffraction studies for ligand **L2** and complexes **Ni3**, **Co1**, **Co3** and **Fe2** were carried out on a Rigaku RAXIS Rapid IP diffractometer with graphite-monochromated Mo Kα radiation (λ = 0.71073 Å). Cell parameters were obtained by global refinement of the positions of all collected reflections. Intensities were corrected for Lorentz and polarization effects and empirical absorption. The structures were solved by direct methods and refined by full-matrix least squares of $F2$. All non-hydrogen atoms were refined anisotropically. The ^{t}Bu group in **Co3** is partly disordered. Structure solution and refinement were performed using the SHELXL-97 package [89]. Crystal data and processing parameters for **L2**, **Ni3**, **Co1**, **Co3 and Fe2** are summarized in Table 7.

Appendix A. Supplementary material

CCDC 699431, 699432, 699433, 699434 and 699435 contains the supplementary crystallographic data for **L2**, **Ni3**, **Co1**, **Co3** and **Fe2**, respectively. These data can be obtained free of charge from The Cambridge Crystallographic Data Centre via www.ccdc.cam.ac.uk/data_request/cif. Supplementary data associated with this article can be found, in the online version, at doi:10.1016/j.jorganchem.2008.09.046.

References

[1] D. Vogt, in: B. Cornils, W.A. Herrmann (Eds.), Applied Homogeneous Catalysis with Organometallic Compounds, vol. 1, Springer, Berlin, 2000, pp. 240–253.
[2] G.W. Parshall, S.D. Ittel (Eds.), Homogeneous Catalysis: The Applications and Chemistry of Catalysis by Soluble Transition Metal Complexes, Wiley, New York, 1992, pp. 68–72.
[3] J. Skupinska, Chem. Rev. 91 (1991) 613–648.
[4] W. Keim, F.H. Kowaldt, R. Goddard, C. Krüger, Angew. Chem. Int. Ed. Engl. 17 (1978) 466–467.
[5] W. Keim, A. Behr, B. Limbäcker, C. Krüger, Angew. Chem. Int. Ed. Engl. 22 (1983) 503.
[6] W. Keim, Angew. Chem. Int. Ed. Engl. 29 (1990) 235–244.
[7] P. Braunstein, Y. Chauvin, S. Mercier, L. Saussine, A.D. Cian, J. Fisher, J. Chem. Soc. Chem. Commun. (1994) 2203–2204.
[8] J. Heinicke, M. He, A. Dal, H.-F. Klein, O. Hetche, W. Keim, U. Flörke, H.-J. Haupt, Eur. J. Inorg. Chem. (2000) 431–440.
[9] P. Braunstein, Y. Chauvin, S. Mercier, L. Saussine, C. R. Chim. 8 (2005) 31–38.
[10] L.K. Johnson, C.M. Killian, M. Brookhart, J. Am. Chem. Soc. 117 (1995) 6414–6415.
[11] B.L. Small, M. Brookhart, A.M.A. Bennett, J. Am. Chem. Soc. 120 (1998) 4049–4050.
[12] G.J.P. Britovsek, V.C. Gibson, B.S. Kimberley, P.J. Maddox, S.J. McTavish, G.A. Solan, A.J.P. White, D.J. Williams, Chem. Commun. (1998) 849–850.
[13] N.A. Cooley, S.M. Green, D.F. Wass, Organometallics 20 (2001) 4769–4771.
[14] Z. Guan, W.J. Marshall, Organometallics 21 (2002) 3580–3586.
[15] G. Mora, S. Zutphen, C. Klemps, L. Ricard, Y. Jean, P.L. Floch, Inorg. Chem. 46 (2007) 10365–10371.
[16] C. Wang, S. Friedrich, T.R. Younkin, R.T. Li, R.H. Grubbs, D.A. Bansleben, M.W. Day, Organometallics 17 (1998) 3149–3151.
[17] T.R. Younkin, E.F. Connor, J.I. Henderson, S.K. Friedrich, R.H. Grubbs, D.A. Bansleben, Science 287 (2000) 460–462.
[18] L. Wang, W.-H. Sun, L. Han, Z. Li, Y. Hu, C. He, C. Yan, J. Organomet. Chem. 650 (2002) 59–64.
[19] T. Hu, L.-M. Tang, X.-F. Li, Y.-S. Li, N.-H. Hu, Organometallics 24 (2005) 2628–2632.
[20] W.-H. Sun, W. Zhang, T. Gao, X. Tang, L. Chen, Y. Li, X. Jin, J. Organomet. Chem. 689 (2004) 917–929.
[21] Q. Shi, S. Zhang, F. Chang, P. Hao, W.-H. Sun, C. R. Chim. 10 (2007) 1200–1208.
[22] W. Keim, S. Killat, C.F. Nobile, G.P. Suranna, U. Englert, R. Wang, S. Mecking, D.L. Schröder, J. Organomet. Chem. 662 (2002) 150–171.
[23] W.-H. Sun, Z. Li, H. Hu, B. Wu, H. Yang, N. Zhu, X. Leng, H. Wang, New J. Chem. 26 (2002) 1474–1478.
[24] F. Speiser, P. Braunstein, L. Saussine, R. Welter, Organometallics 23 (2004) 2613–2624.
[25] X. Tang, D. Zhang, S. Jie, W.-H. Sun, J. Chen, J. Organomet. Chem. 690 (2005) 3918–3928.
[26] Z. Weng, S. Teo, T.S.A. Hor, Organometallics 25 (2006) 4878–4882.
[27] A. Kermagoret, P. Braunstein, Organometallics 27 (2008) 88–99.
[28] C.M. Killian, D.J. Tempel, L.K. Johnson, M. Brookhart, J. Am. Chem. Soc. 118 (1996) 11664–11665.
[29] S.A. Svejda, M. Brookhart, Organometallics 18 (1999) 65–74.
[30] B.Y. Lee, X. Bu, G.C. Bazan, Organometallics 20 (2001) 5425–5431.
[31] C. Shao, W.-H. Sun, Z. Li, Y. Hu, L. Han, Cat. Commun. 3 (2002) 405–410.
[32] X. Tang, W.-H. Sun, T. Gao, J. Hou, J. Chen, W. Chen, J. Organomet. Chem. 690 (2005) 1570–1580.
[33] S. Jie, D. Zhang, T. Zhang, W.-H. Sun, J. Chen, Q. Ren, D. Liu, G. Zheng, W. Chen, J. Organomet. Chem. 690 (2005) 1739–1749.
[34] J.M. Benito, E. de Jesús, F.J. de la Mata, J.C. Flores, F. Gómez, P. Gómez-Sal, Organometallics 25 (2006) 3876–3887.
[35] C.-L. Song, L.-M. Tang, Y.-G. Li, X.-F. Li, J. Chen, Y.S. Li, J. Polym. Sci., Part A: Polym. Chem. 44 (2006) 1964–1974.
[36] L. Wang, C. Zhang, Z.-X. Wang, Eur. J. Inorg. Chem. (2007) 2477–2487.
[37] B.K. Bahuleyan, G.W. Son, D.-W. Park, C.-S. Ha, I. Kim, J. Polym. Sci. Part A: Polym. Chem. 46 (2008) 1066–1082.
[38] M. Tanabiki, K. Tsuchiya, Y. Kumanomido, K. Matsubara, Y. Motoyama, H. Nagashima, Organometallics 23 (2004) 3976–3981.
[39] M. Tanabiki, K. Tsuchiya, Y. Motoyama, H. Nagashima, Chem. Commun. (2005) 3409–3411.
[40] Q.-Z. Yang, A. Kermagoret, M. Agostinho, O. Siri, P. Braunstein, Organometallics 25 (2006) 5518–5527.
[41] F. Speiser, P. Braunstein, L. Saussine, Dalton Trans. (2004) 1539–1545.
[42] J. Hou, W.-H. Sun, S. Zhang, H. Ma, Y. Deng, X. Lu, Organometallics 25 (2006) 236–244.
[43] C. Zhang, W. -H. Sun, Z.-X. Wang, Eur. J. Inorg. Chem. (2006) 4895–4902.
[44] B.L. Small, M. Brookhart, J. Am. Chem. Soc. 120 (1998) 7143–7144.
[45] S. Al-Benna, M.J. Sarsfield, M. Thornton-Pett, D.L. Ormsby, P.J. Maddox, P. Brès, M. Bochmann, J. Chem. Soc. Dalton Trans. (2000) 4247–4257.
[46] F.A. Kunrath, R.F. De Souza, O.L. Casagrande Jr, N.R. Brooks, V.G. Young Jr, Organometallics 22 (2003) 4739–4743.
[47] R. Cowdell, C.J. Davies, S.J. Hilton, J.-D. Maréchal, G.A. Solan, O. Thomas, J. Fawcett, Dalton Trans. (2004) 3231–3240.
[48] N. Ajellal, M.C.A. Kuhn, A.D.G. Boff, M. Hörner, C.M. Thomas, J.-F. Carpentier, O.L. Casagrande, Organometallics 25 (2006) 1213–1216.
[49] F. Kaul, G. Puchta, G. Frey, E. Herdtweek, W. Herrmann, Organometallics 26 (2007) 988–999.
[50] G.J.P. Britovsek, M. Bruce, V.C. Gibson, B.S. Kimberley, P.J. Maddox, S. Mastroianni, S.J. McTavish, C. Redshaw, G.A. Solan, S. Strömberg, A.J.P. White, D.J. Williams, J. Am. Chem. Soc. 121 (1999) 8728–8740.
[51] S. Fernandes, R.M. Bellabarba, D.F. Ribeiro, P.T. Gomes, J.R. Ascenso, J.F. Mano, A.R. Dias, M.M. Marques, Polym. Int. 51 (2002) 1301–1303.
[52] W.-H. Sun, S. Zhang, W. Zuo, C. R. Chim. 11 (2008) 307–316.
[53] L. Wang, W.-H. Sun, L. Han, H. Yang, Y. Hu, X. Jin, J. Organomet. Chem. 658 (2002) 62–70.
[54] W.-H. Sun, S. Jie, S. Zhang, W. Zhang, Y. Song, H. Ma, J. Chen, K. Wedeking, R. Fröhlich, Organometallics 25 (2006) 666–677.
[55] W.-H. Sun, S. Zhang, S. Jie, W. Zhang, Y. Li, H. Ma, J. Chen, K. Wedeking, R. Fröhlich, J. Organomet. Chem. 691 (2006) 4196–4203.
[56] S. Jie, S. Zhang, W.-H. Sun, X. Kuang, T. Liu, J. Guo, J. Mol. Catal. A: Chem. 269 (2007) 85–96.
[57] S. Zhang, S. Jie, Q. Shi, W.-H. Sun, J. Mol. Catal. A: Chem. 276 (2007) 174–183.
[58] S. Jie, S. Zhang, W.-H. Sun, Eur. J. Inorg. Chem. (2007) 5584–5598.
[59] W.-H. Sun, P. Hao, S. Zhang, Q. Shi, W. Zuo, X. Tang, Organometallics 26 (2007) 2720–2734.
[60] P. Hao, S. Zhang, W.-H. Sun, Q. Shi, S. Adewuyi, X. Lu, P. Li, Organometallics 26 (2007) 2439–2446.
[61] Y. Chen, P. Hao, W. Zuo, K. Gao, W.-H. Sun, J. Organomet. Chem. 693 (2008) 1829–1840.
[62] W.-H. Sun, P. Hao, G. Li, S. Zhang, W. Wang, J. Yi, M. Asma, N. Tang, J. Organomet. Chem. 692 (2007) 4506–4518.
[63] S. Adewuyi, G. Li, S. Zhang, W. Wang, P. Hao, W.-H. Sun, N. Tang, J. Yi, J. Organomet. Chem. 692 (2007) 3532–3541.
[64] S. Zhang, I. Vystorop, Z. Tang, W.-H. Sun, Organometallics 26 (2007) 2456–2460.
[65] S. Zhang, W.-H. Sun, X. Kuang, I. Vystorop, J. Yi, J. Organomet. Chem. 692 (2007) 5307–5316.
[66] M. Zhang, S. Zhang, P. Hao, S. Jie, W.-H. Sun, P. Li, X. Lu, Eur. J. Inorg. Chem. (2007) 3816–3826.
[67] M. Zhang, P. Hao, W. Zuo, S. Jie, W.-H. Sun, J. Organomet. Chem. 693 (2008) 483–491.
[68] C. Bianchini, G. Mantovani, A. Meli, F. Migliacci, F. Laschi, Organometallics 22 (2003) 2545–2547.
[69] C. Bianchini, G. Giambastiani, G. Mantovani, A. Meli, D. Mimeau, J. Organomet. Chem. 689 (2004) 1356–1361.
[70] C. Bianchini, D. Gatteschi, G. Giambastiani, I.G. Rios, A. Ienco, F. Laschi, C. Mealli, A. Meli, L. Sorace, A. Toti, F. Vizza, Organometallics 26 (2007) 726–739.
[71] R. Gao, L. Xiao, X. Hao, W.-H. Sun, F. Wang, Dalton Trans. (2008) 5645–5651.
[72] R. Gao, M. Zhang, T. Liang, F. Wang, W.-H. Sun, Organometallic 2008, doi:10.1021/om800647w.
[73] P. Belser, S. Bernhard, U. Guerig, Tetrahedron 52 (1996) 2937–2944.
[74] C.J. Chandler, L.W. Deady, J.A. Reiss, J. Heterocyclic. Chem. 18 (1981) 599–601.
[75] R.A. Poole, G. Bobba, M.J. Cann, J.-C. Frias, D. Parker, R.D. Peacock, Org. Biomol. Chem. 3 (2005) 1013–1024.
[76] M. Ishihara, H. Togo, Tetrahedron 63 (2007) 1474–1480.
[77] F.C. Schaefer, G.A. Peters, J. Org. Chem. 26 (1961) 412–418.
[78] S. Gladiali, L. Pinna, G. Delogu, E. Graf, H. Bruuner, Tetrahedron: Asymmetry. 1 (1990) 937–942.
[79] F. Speiser, P. Braunstein, L. Saussine, Organometallics 23 (2004) 2633–2640.
[80] N. Ajellal, M.C.A. Kuhn, A.D.G. Boff, M. Hörner, C.M. Thomas, J.-F. Carpentier, O.L. Casagrande Jr., Organometallics 25 (2006) 1213–1216.
[81] D. Guo, L. Han, T. Zhang, W.-H. Sun, T. Li, X. Yang, Macromol. Theory Simul. 11 (2002) 1006–1012.
[82] W.-H. Sun, X. Tang, T. Gao, B. Wu, W. Zhang, H. Ma, Organometallics 23 (2004) 5037–5047.
[83] T. Zhang, D. Guo, S. Jie, W.-H. Sun, T. Li, X. Yang, J. Polym. Sci. Part A: Polym. Chem. 42 (2004) 4765–4774.
[84] E.Y. Chen, T.J. Marks, Chem. Rev. 100 (2000) 1391–1434.
[85] A.R. Karam, E.L. Catarí, F. López-Linares, G. Agrifoglio, C.L. Albano, A. Díaz-Barrios, T.E. Lehmann, S.V. Pekerar, L.A. Albornoz, R. Atencio, T. González, H.B. Ortega, P. Joskowics, Appl. Catal. A: Gen. 280 (2005) 165–173.
[86] G.J.P. Britovsek, S. Mastroianni, G.A. Solan, S.P.D. Baugh, C. Redshaw, V.C. Gibson, A.J.P. White, D.J. Williams, M.R.J. Elsegood, Chem. Eur. J. 6 (2000) 2221–2231.
[87] D.J. Greighton, J. Hajdu, D.S. Sigman, J. Am. Chem. Soc. 98 (1976) 4619–4624.
[88] E.J. Corey, A.L. Borror, T. Foglia, J. Org. Chem. 30 (1965) 288–290.
[89] G. M. Sheldrick, SHELXL-97, Program for the Refinement of Crystal Structures, University of Göttingen, Germany, 1997.